Geoneutrinos

L. Ludhova
Institut für Kernphysik, Forschungszentrum Jülich, 52425 Jülich, Germany
and
RWTH Aachen University, 52062 Aachen, Germany

Geoneutrinos, antineutrinos released in decays of long-lived radioactive elements inside the Earth, represent unique direct messengers about the amount of the Earth's radiogenic heat. The newly born neutrino geoscience, a truly inter-disciplinary field of neutrino physicists and geo-scientists, is an excellent example of how the progress in one research area can bring profit to another field. The extremely challenging neutrino detection is now added among the geological methods how to study the deep layers of our planet. The large–volume liquid–scintillator detectors, originally built to measure neutrinos or anti-neutrinos from other sources, are capable to detect geoneutrinos, as it was demonstrated by KamLAND (Japan) and Borexino (Italy) experiments. All together, less than 200 geoneutrinos have been detected so far. In order to fully exploit the potential of geoneutrinos, the next generation of large-volume detectors, possibly located in well optimized locations, is needed. Several future projects as SNO+, JUNO or Jinping have geoneutrino measurements among their scientific goals. This work tries to follow the development of this field, from the first ideas to exploit geoneutrinos for understanding of our planet, through the existing measurements, up to the outlook and future prospects of this new field.

1 What are geoneutrinos and why to study them

People witness demonstrations of the enormous power hidden in the depth of our Earth since millennia. Sometimes destructive, sometimes spectacular, sometimes vital for the evolution of life: we can mention earthquakes, volcanic eruptions, but also curative hot springs, geothermal energy and even the movement of lithospheric plates. Geoscientists are trying to answer the question from where is coming the energy driving these processes. And today, neutrino physics can help to understand.

The integrated surface heat flux of the Earth is estimated to be 47 ± 3 TW [1,2], based on the measurements of temperature gradients along several thousands bore holes along the globe. The main expected contributions to this heat, shown in diagram of Fig. 1, are the latent heat from the time of the Earth's accretion and the radiogenic heat. The latter, e.g. the heat released along the decays of long-lived radioactive elements inside the Earth, can be pinned down by detecting geoneutrinos, antineutrinos released in decays of long-lived radioactive elements inside the Earth.

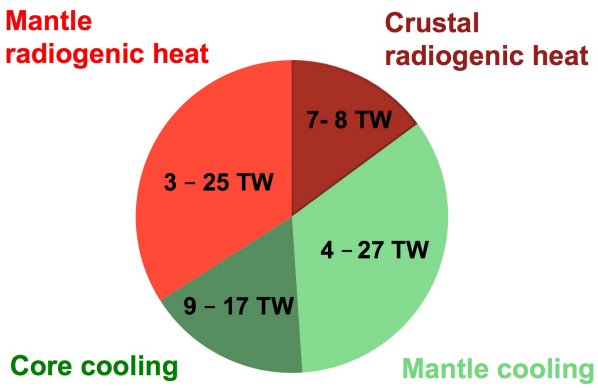

Figure 1 – The estimated contributions of different sources to the integrated Earth's surface heat flux 47 ± 3 TW [1,2]. The radiogenic contribution can be pinned down by geoneutrino measurements.

Today, the Earth's radiogenic heat is in almost 99 % produced along with the radioactive decays in the chains of ^{232}Th ($\tau_{1/2} = 14.0 \cdot 10^9$ yr), ^{238}U (99.2739 % of natural U, $\tau_{1/2} = 4.47 \cdot 10^9$ yr), ^{235}U (0.7205 % of natural U, $\tau_{1/2} = 0.71 \cdot 10^9$ yr), and those of the ^{40}K isotope (0.012 % of natural K, $\tau_{1/2} = 1.28 \cdot 10^9$ yr). The overall decay schemes and the heat released in each of these decays are summarized in the following equations:

$$^{238}\mathrm{U} \rightarrow {}^{206}\mathrm{Pb} + 8\alpha + 8e^- + 6\bar{\nu}_e + 51.7 \quad \mathrm{MeV} \tag{1}$$

$$^{235}\mathrm{U} \rightarrow {}^{207}\mathrm{Pb} + 7\alpha + 4e^- + 4\bar{\nu}_e + 46.4 \ \mathrm{MeV} \tag{2}$$

$$^{232}\mathrm{Th} \rightarrow {}^{208}\mathrm{Pb} + 6\alpha + 4e^- + 4\bar{\nu}_e + 42.7 \ \mathrm{MeV} \tag{3}$$

$$^{40}\mathrm{K} \rightarrow {}^{40}\mathrm{Ca} + e^- + \bar{\nu}_e + 1.31 \ \mathrm{MeV} \ (89.3\%) \tag{4}$$

$$^{40}\mathrm{K} + \mathrm{e} \rightarrow {}^{40}\mathrm{Ar} + \nu_e + 1.505 \ \mathrm{MeV} \quad (10.7\%) \tag{5}$$

Figure 2 demonstrates the interplay between geo-sciences and geoneutrinos. In principle, the abundances of the radioactive elements (or Heat Producing Elements, HPE) inside the Earth and the amount of the released radiogenic heat are strictly correlated "just through the nuclear physics". The estimation of the radiogenic heat inside the Earth, and in particular the radiogenic heat from the deep mantle, from which we do not have any direct rock samples, are the main goal of geoneutrino measurements. However, the information about the HPE distribution inside the Earth is fundamental both for the prediction of the expected geoneutrino flux, as well as for the interpretation of the geoneutrino measurements. It is only through an intense collaboration between geologists and physicists that the new tool can be exploited to its fullest. Among further goals of this new field is the discrimination between the different Bulk Silicate Earth models, testing the mantle homogeneity and stratification, determination of the Earth's bulk U/Th ratio, that would provide insights about the processes of the Earth's formation, or testing the ideas of additional heat sources inside the Earth.

2 The first ideas

The idea to exploit neutrinos emitted in decays of potassium and along the uranium and thorium chains, in order to determine the Earth's radiogenic heat, was first proposed by G. Eder [3] in 1965. His main motivation was to find the heat source for the that-time-expected Earth expansion of 0.8 mm/year. He has also evaluated the expected fluxes to 10^8 cm^{-2} s^{-1}, that is 2 orders of magnitude more than we know them to be today. He also brought up the idea of using the Inverse Beta Decay (IBD):

$$\bar{\nu}_e + p \rightarrow e^+ + n \tag{6}$$

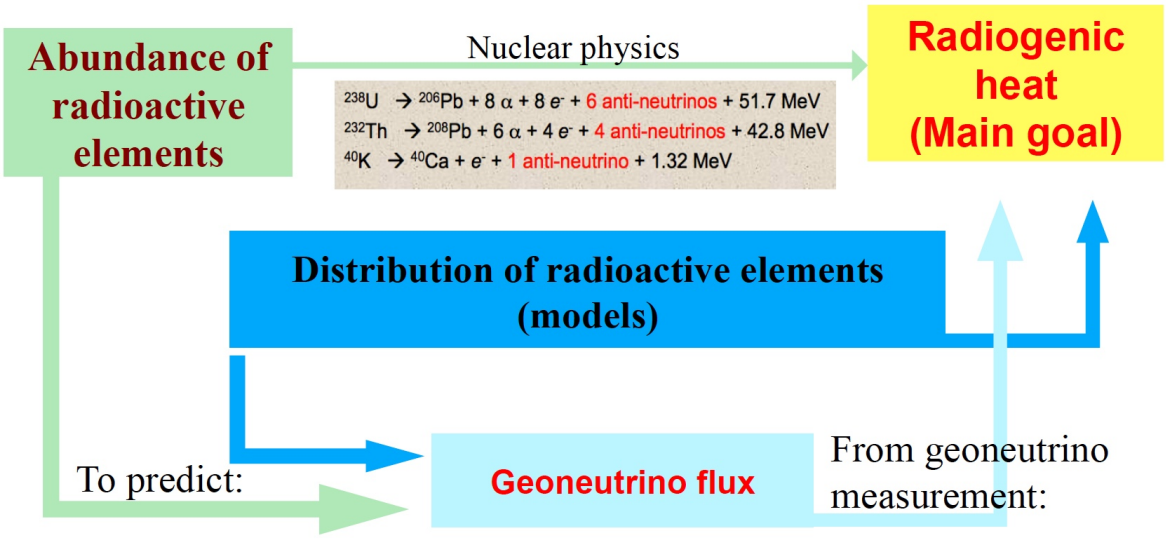

Figure 2 – Neutrino geoscience is a truly inter-disciplinary research field. Details in text.

for their detection and estimated the corresponding interaction rate as 4 positrons per day in 500 tons of water. This reaction, exploitng the delayed coincidence between the positron and the neutron, is actually used today for geoneutrino detection in liquid-scintillator detectors, as it will be described in Sec. 4.

The idea to exploit neutrinos to study the Earth, along with other astronomical objects, was further developed by G. Marx alone [4] and with co-authors [5,6,7]. His estimation of the total geoneutrino flux was of 10^9 cm^{-2} s^{-1}, so still too large with respect to reality. He discussed with more detail possible detection reactions as Inverse Beta Decay on proton, as in Eq. 6, but also on ^{3}He and ^{35}Cl. He also considered the detection of mono-energetic antineutrinos through Induced Electron Capture:

$$\bar{\nu}_e + e^- + X \rightarrow Y \tag{7}$$

on, for example, $X =^{130}$Ba, ^{209}Bi, ^{112}Sn for energies 0.44, 0.63, and 0.65 MeV, respectively.

A much broader discussion concerning both geological motivation of these studies (including composition and dynamics of the Earth) as well as detection methods was presented by L.M. Krauss, S. L. Glashow, and D. N. Schramm [8] in 1984. The expected geoneutrino flux of 10^7 cm^{-2} s^{-1} approaches the realistic values. Very detailed is the discussion of radiochemical detection methods exploiting both IBDs as well as Induced Electron Capture reactions.

R. Raghavan played a key role in pioneering ideas how to exploit liquid–scintillator detectors in neutrino detection. He discussed in an internal report the detection of a possible nuclear fission reactor at the center of the Earth [9]. With the co-authors from both Borexino and KamLAND experiments, he discussed "Measuring the global radioactivity in the Earth by multi-detector anti-neutrino spectroscopy" in 1998 [10]. The idea of using liquid–scintillator detectors for "antineutrino geophysics" is also discussed by C. G. Rothschild, M. C. Chen, and F. P. Calaprice in the same year [11]. This method of using the IBD interaction on proton, as in Eq. 6, in liquid–scintillator detectors was proven to be successful, as it will be described below.

3 Expected geoneutrino flux today

In this section we describe the current approaches in the evaluation of the expected geoneutrino flux at different locations on the Earth's surface, as at the experimental sites of the current and future geoneutrino detectors. In this matter, it is fundamental to introduce the concept of Bulk Silicate Earth (BSE) models. These models predict the abundances of chemical elements, including HPE as sources of geoneutrinos, in the Earth's primitive mantle. The primitive mantle

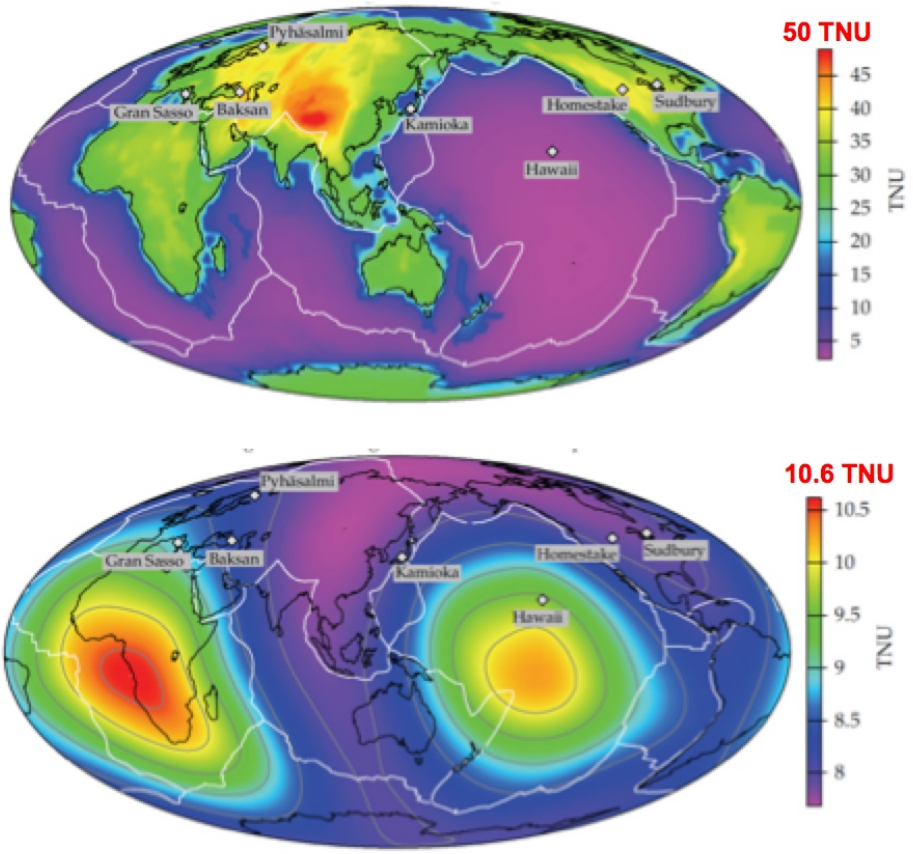

Figure 3 – Expected geoneutrino signal [42] expressed in the TNU units from the crust (top) and from the mantle (bottom). The latter in a hypothesis of heterogeneous mantle, motivated by the Large Shear Velocity Provinces [43] observed at the mantle base below Africa and Pacific ocean.

is called the silicate Earth that existed after the segregation of the Earth's metallic core and before the differentiation of the present-day mantle and crust. Thus, in the first approximation, the HPE abundances (or radiogenic heat) predicted by the BSE models can be considered as the sum of the abundances (or radiogenic heat) in the present-day mantle and crust. Since we have much more direct rock samples and information in general about the curst with respect to the mantle, our estimation of the total radiogenic heat from the crust is more precise. We expect only about 0.2 TW from the thin and HPE not-so-rich oceanic crust, while about 7-8 TW from the more complex, thicker, and HPE enriched continental crust [12,13,14,15,16,17].

The BSE models take into account a broad spectrum of inputs, as for example the composition of chondritic meteorites and its correlation with the composition of the solar photosphere, composition of the rock samples from the upper mantle or from the Mid-Ocean Ridge Basalts (MORB), the energy needed to run the convection of the mantle etc. There is a very broad spectrum of different BSE models [18,19,20,21,22,23,24,25,26,27,28,29,30]. Considering the spread of the BSE-predicted HPE abundances, after the subtraction of the relatively well known crustal heat of 7-8 TW, the expected radiogenic heat from the mantle appears to be in a broad interval from 3 to 25 TW. To pin down this contribution is the main goal of geoneutrino studies.

In order to predict the geoneutrino flux at some location, one has to "know" or has to assume some approximations concerning the HPE abundances and distributions. Knowing those, one has to "simply integrate" over the Earth and consider the effect of neutrino oscillations. The latter, in the first approximation, can be considered as not deforming the shape of geoneutrino energy

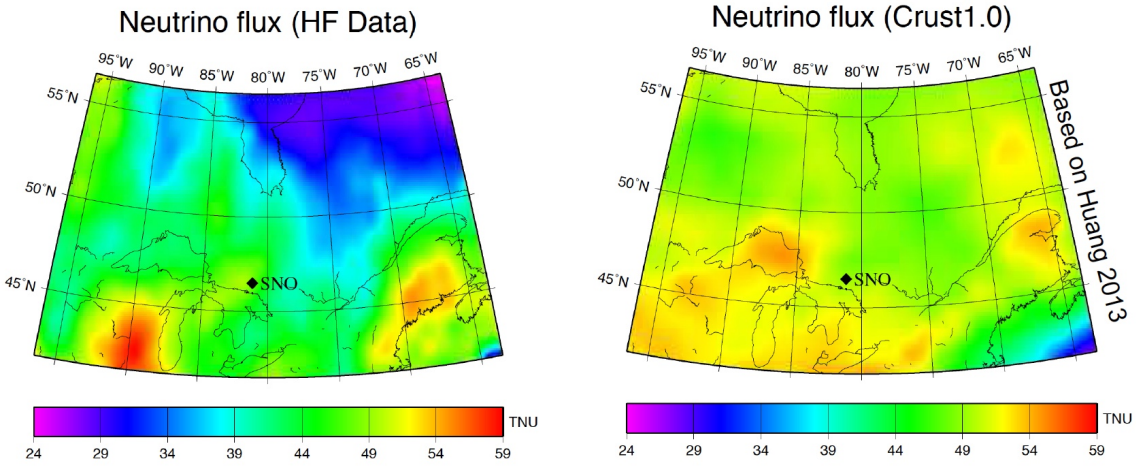

Figure 4 – Expected geoneutrino signal expressed in TNU units [46] calculated for the craton area around the SNO laboratory in Canada. The left plot shows the expected signal based on the heat flow measurements, while the right plot shows the expectations based on the U and Th abundances from the Crust 1.0 model.

spectrum, only reducing the overall flux of electron-flavour to about 54%. In this terms, the works of the group of G. Fiorentini and F. Mantovani have to be underlined [31,32,33]. On the continental crust, the area of few-hundreds-km diameter contributes up to 50% to the total geoneutrino signal. In this area of the so-called Local Crust (LOC), one has to know the detailed geological structure and realistic compositions of different rock types that are present around the site. A lot of work has been done in this matter, concerning the estimation of the LOC contributions around the KamLAND, Borexino, SNO, JUNO, Jinping sites [34,35,36,37,38,39]. For the further-away Rest Of the Crust (ROC), some approximations can be made. The crust is divided in finite volume voxels (3D bins) with surface area of either $5^\circ \times 5^\circ$ [11], $2^\circ \times 2^\circ$ [40,41,32] or, most recently, $1^\circ \times 1^\circ$ [17]. The oceanic and continental crusts are treated separately. The continental crust is further divided in different layers, as upper, middle, and lower continental crust. The calculation of the mantle contribution has then to be based on a selected BSE model, from which the crustal contribution is subtracted and some assumptions about the distribution of the remaining HPE in the mantle are made.

An example of a similar calculation [42] of the expected geoneutrino signal on the Earth's surface is shown in Fig. 3 separately for the crust (top) and the mantle (bottom). It is expressed in the so called Terrestrial Neutrino Unit (TNU), defined as the number of IBD interactions detected during one year on a target of 10^{32} protons ($\sim$1 kton of liquid scintillator) and with 100% detection efficiency. As it can be seen, the expected geoneutrino signal is small. Even in the Himalaya area, where the continental crust is the thickest (about 70 km), the expected crustal signal is around 50 TNU. On the oceanic crust, the signal does not exceed 10 TNU. This underlines the need of large detectors and the fact that the determination of the mantle contribution is even more challenging.

An alternative approach to the estimation of geoneutrino signal is based on the heat–flux measurements. This approach is being developed by the groups around C. Jaupart, J.-C. Mareschal, H. K. C. Perry [44,45]. Figure 4 compares the predicted geoneutrino signal calculated [46] for the craton area around the SNO laboratory in Canada. The left plot shows the expected signal based on the heat–flow measurements, while the right plot shows the expectations based on the U and Th abundances from the Crust 1.0 model.

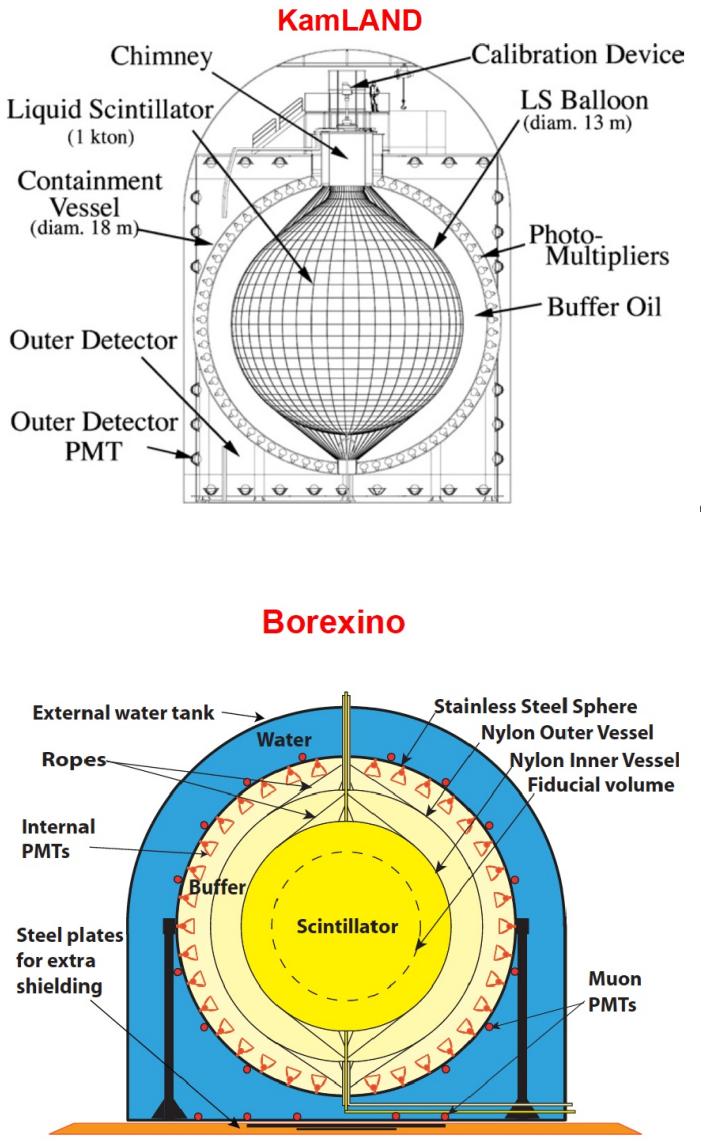

Figure 5 – Schemes of the KamLAND (top) and the Borexino (bottom) detectors.

4 From the first geoneutrino detection up to the most recent results

Today, only two experiments, KamLAND [47] and Borexino [48], succeeded to measure geoneutrinos. Both are large-volume liquid-scintillator (LS) detectors, schematically shown in Fig. 5, placed underground in order to shield from cosmic radiation and constructed from highly radio-pure materials. KamLAND is located in the Kamioka mine in Japan, at a border between oceanic and continental crusts. It has about 1000 ton of LS-target and is taking data since 2002. Its main goal was the measurement of reactor antineutrinos and the observation of neutrino oscillations. Borexino instead, placed at Laboratori Nazionali del Gran Sasso in Italy and on the continental crust, is taking data since 2007 with 280 ton LS-target. Borexino main goal is the measurement of solar neutrinos through elastic scattering of electrons, and thus much higher radio-purity of the LS has been required and achieved. This means that in Borexino, the non-antineutrino background in the IBD detection channel has been almost completely suppressed.

The hydrogen nuclei that are copiously present in hydrocarbon (C_nH_{2n}) LS detectors act as target for electron antineutrinos in the IBD reaction already shown in Eq. 6. Since the produced neutron is heavier than target proton, the IBD interaction has a kinematic threshold of 1.8 MeV. In this process, a positron and a neutron are emitted as reaction products. The positron promptly

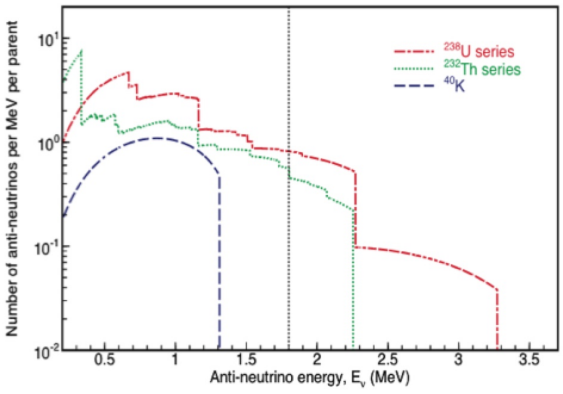

Figure 6 – The expected spectrum of geoneutrinos emitted per 1 fission of mother nuclei of ^{238}U (red), ^{232}Th (green), and ^{40}K (blue). The vertical line shows the 1.8 MeV kinematic threshold of the IBD interaction used today in LS-based detectors.

comes to rest and annihilates emitting two 511 keV γ-rays, yielding a *prompt event*, with a visible energy E_{prompt}, directly correlated with the incident antineutrino energy $E_{\bar{\nu}_e}$:

$$E_{prompt} \sim E_{\bar{\nu}_e} - 0.784 MeV, \tag{8}$$

in which the offset results mosly from the difference between the 1.8 MeV, absorbed from $E_{\bar{\nu}_e}$ in order to make the IBD kinematically possible, and the energy released during the positron annihilation. The emitted neutron keeps initially the information about the $\bar{\nu}_e$ direction, but, unfortunately, it is typically captured on protons only after a quite long thermalization time (τ = 200 - 250 μs, depending on scintillator). During this time, the directionality memory is lost in many scattering collisions. When the thermalized neutron is captured on proton, it gives a typical 2.22 MeV de-excitation γ-ray, which provides a coincident *delayed event*. The pairs of time and spatial coincidences between the prompt and the delayed signals offer a clean signature of $\bar{\nu}_e$ interactions, very different from the ν_e scattering process used in the neutrino detection.

The expected spectra of geoneutrinos from the decays of ^{40}K and from the chains of ^{238}U and ^{232}Th are shown in Fig. 6. Note that ^{40}K geoneutrinos cannot be detected with present-day detection technique, since the corresponding energy spectrum lies fully below the IBD threshold of 1.8 MeV.

The coincidence tag used in the electron antineutrino detection is a very powerful tool in background suppression. The main antineutrino background in the geo-neutrino measurements results from nuclear power plants. Considering the known composition of reactor cores, their thermal powers, geographical positions, and the known energy spectra of antineutrinos emitted from fissions of ^{235,238}U and ^{239,241}Pu isotopes, the expected reactor spectra can be calculated with the precision largely exceeding the one of the current geoneutrino measurements [49]. Other, non-antineutrino background sources can arise from intrinsic detector contaminations, as from random coincidences of non-correlated events and from (α, n) reactions, in which α's are mostly due to the ^{210}Po decay (belonging to the ^{238}U chain) and from cosmogenic sources, mostly residual muons and muon–induced neutrons and unstable nuclides like ^{9}Li and ^{8}He having an (β + neutron) decay branch, perfectly mimicking IBD interaction. The non-antineutrino backgrounds can be studied independently and constrained in the final geoneutrino analysis. Random coincidences can be determined with high statistical precision by studying the off-time correlation window. The rate of the (α, n) background can be estimated based on the measured contamination of the LS with ^{210}Po which α-decays can be recognized on event-by-event basis thanks to the pulse-shape discrimination techniques. Finally, the rate of cosmogenic backgrounds can be estimated by studying the muon detection efficiency and the cosmogenic background detected after muons within the muon veto times.

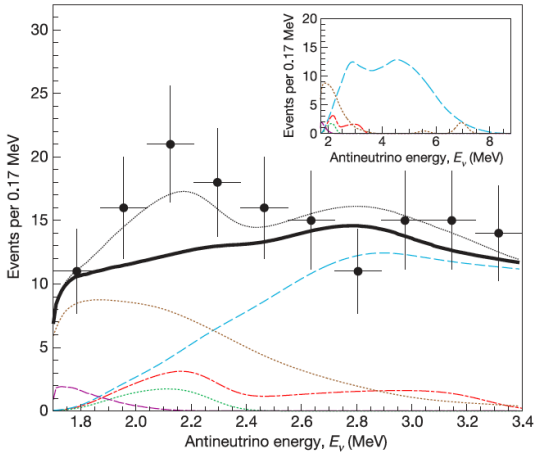

Figure 7 – Antineutrino energy spectrum in KamLAND: the first investigation of geoneutrinos performed in 2005 [51]. The thick solid black line shows the best fit without geoneutrino component, while the thin black solid line shows the final best fit with geoneutrinos included.

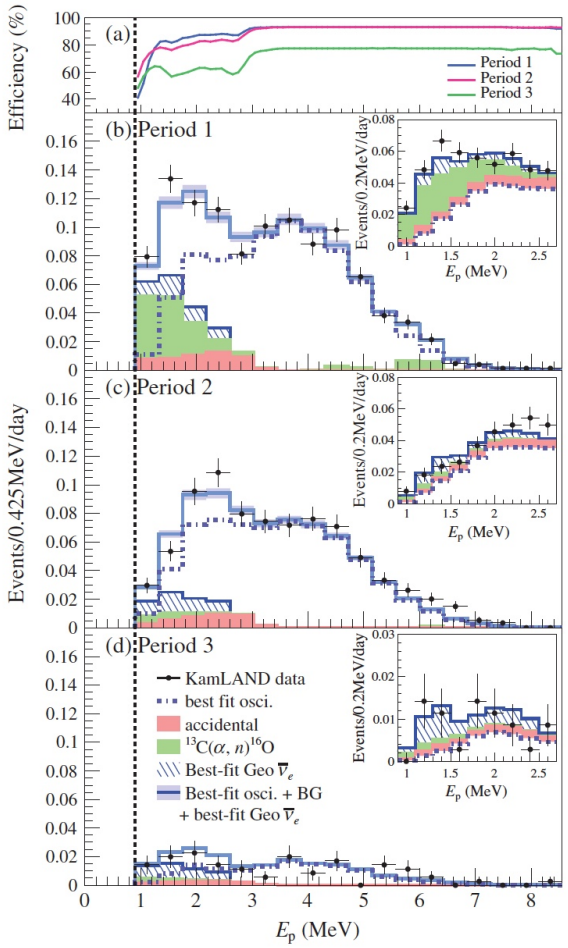

Figure 8 – Prompt energy spectra of anti-neutrino candidate events above 0.9 MeV energy threshold for 3 KamLAND data taking periods [54]. The prompt energy spectra of candidates in the geoneutrino energy window are also shown in the insets with a finer binning. Details in the text.

KamLAND was the first experiment to perform experimental investigation of geo-neutrinos in 2005 [50,51]. The corresponding spectrum of antineutrino candidates and the best fit demonstrating the presence of geoneutrino signal at about 2σ C.L. is shown in Fig. 7. An updated geo-neutrino analysis was released in 2008 [52]. An extensive liquid-scintillator purification campaign to improve

its radio-purity took place in years 2007 - 2009. Consequently, a new geo-neutrino observation at 99.997% C.L. was achieved in 2011 with an improved signal-to-background ratio [53]. After the earthquake and the consequent Fukushima nuclear accident occurred in March 2011, all Japanese nuclear reactors were temporarily switched off for a safety review. Such situation allowed for a reactor on-off study of backgrounds and also yielded an improved sensitivity for $\bar{\nu}_e$ produced by other sources, like geo-neutrinos. A new result on geo-neutrinos has been released in 2013 [54]. Figure 8 shows the KamLAND antineutrino spectra (geoneutrino contribution is shown in blue-dashed area) in the three different periods: on the top, Period 1 (2002-2007) before the LS purification with large amount of reactor, accidental, and (α, n) background; in the middle, Period 2 (2009-2011) after the LS-purification, with the non-antineutrino background strongly suppressed; in the bottom, Period 3 (after the 2011 Fukushima event), with further strong reduction of reactor antineutrino background. The best fit of the total spectrum shown in Fig. 9 yields 116^{+28}_{-27} geoneutrinos detected with 4.9×10^{32} target-proton $\times$ year exposure. KamLAND has released a preliminary result in 2016 on a conference talk [55] including the low-background data until 2016. The best fit yielded 164^{+28}_{-25} geoneutrinos with 6.39×10^{32} target-proton $\times$ year exposure.

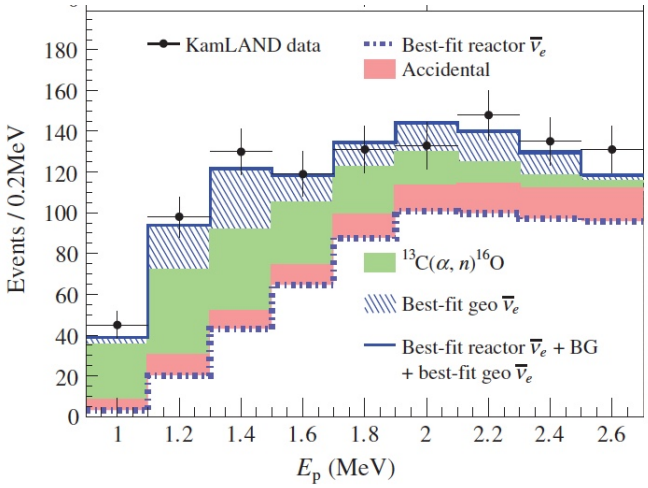

Figure 9 – Prompt energy spectrum of the KamLAND anti-neutrino candidates in the geoneutrino energy window for all data-taking periods Periods 1-3 [54]. The geoneutrino contribution is shown in blue-dashed area.

Borexino published its first observation of geoneutrinos in 2010 [56] by observing $9.9^{+4.1}_{-3.4}$ geoneutrinos. The relatively high 99.997% C.L. observation was achieved with relatively small exposure of 1.5×10^{31} target-proton $\times$ year, thanks to almost negligible non-antineutrino background of (0.14 ± 0.02) events and relatively small reactor anti-neutrino background, since Italy does not have any nuclear power plant in operation. Borexino provided an update in 2013 [57] and in 2015 [58]. The latest Borexino antineutrino spectrum and the best fit are shown in Fig. 10. Within the exposure of $(5.5 \pm 0.3) \times 10^{31}$ target-proton $\times$ year, $23.7^{+6.5}_{-5.7}(\text{stat})^{+0.9}_{-0.6}(\text{sys})$ geoneutrino events have been detected. The null observation of geoneutrinos has a probability of 3.6×10^{-9} (5.9σ).

The measured geoneutrino signals are in agreement with expectations based on the geological models. This is a remarkable achievement of both geosciences, being able to model the composition of the deep layers of our planet, as well as of neutrino physics, being able to measure the faint geoneutrino signal. However, due to the large error of the existing geoneutrino measurements, it is not possible to distinguish among different BSE models. By performing the fits with free U and Th contributions, we obtain the U/Th ratio compatible with its chondritic value, but the errors are still too big to proceed with firm interpretations. The first indications of the observation of the mantle signal appear, as for example at 98% confidence level by Borexino [58]. Some exotic ideas, as for example the presence of an Uranium geo-reactor with a typical power of 3-10 TW at the Earth's core [59], have been practically excluded by both Borexino and KamLAND measurements.

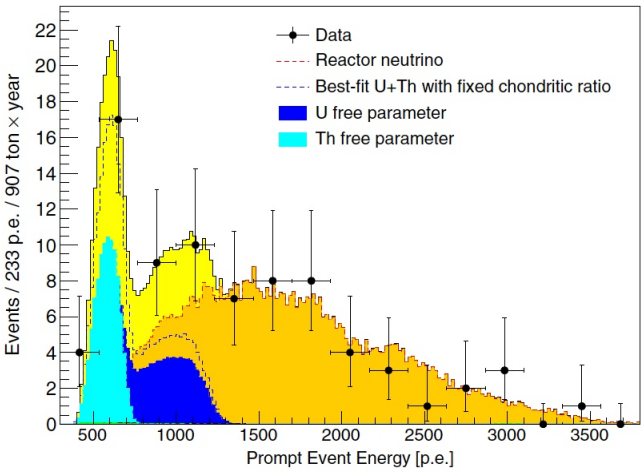

Figure 10 – Prompt-yield spectrum in units of photoelectrons (p.e.) (1 MeV corresponds to about 500 p.e.), of anti-neutrino candidates from Borexino latest release in 2015 [58]. The best-fit shows the total contribution of geoneutrino (assuming the chondritic U and Th ratio) and backgrounds (reactor neutrino in orange colored area, non-antineutrino background is in green, almost non-visible at the lowest energy region). The result of a separate fit with U (blue colored area) and Th (light-blue colored area) set as free and independent parameters is also shown.

5 Neutrino geoscience: outlook

The new field of Neutrino Geoscience has been born and an inter-disciplinary community of physicists and geoscientists is developing. The first geoneutrino results confirm the feasibility of these measurements. The measured rates are in agreement with the expectations, confirming that at this level of precision we have a good understanding of our Earth. However, there is a potential to learn more about our planet from geoneutrinos and we should take this chance and invest in the next generation of the experiments providing new more precise results. We need more and possibly high statistics data. This means building the next generation of multi-kton detectors. Obtaining results from the multi-site experiments can help in testing the homogeneity of the mantle composition. Building the detectors at geologically strategic positions would help, for example, to pin down the mantle radiogenic heat contribution to the total Earth's heat budget.

What can we expect in the next future? Borexino continues to take data and a new update with about 20% precision is to be released. Also KamLAND is preparing a new release with further data with extremely low background levels with still majority of Japanese nuclear reactors switched off.

From the future projects, the SNO+ experiment [60], 1 kton liquid scintillator detector in Sudbury mine in Canada, is starting its data taking, having geoneutrinos among its goals. Geoneutrinos are of a great interest also for JUNO [61], the first multi-kton liquid scintillator detector under construction in Jiangmen, China. With its 20 kton target mass, it will get into operation in 2021. Its main goal is the determination of neutrino mass hierarchy by measurement of reactor antineutrinos with 53 km baseline. Inevitable disadvantage of the large reactor antineutrino background and a relatively shallow depth, are both balanced by the detector large size and an excellent energy resolution of 3% at 1 MeV. The expected number of geoneutrino events is about 400/year. Within the first years, JUNO geoneutrino measurement will quickly exceed the precision of current geoneutrino results.

From the experiments under consideration, one has to mention the Jinping neutrino experiment [62]. It would be a few kton LS or slow-LS based detector placed in the world's deepest underground laboratory, far away from any nuclear power plant in the Himalaya region.

A real breakthrough in this field would come with the proposed Hanohano [63] project in Hawaii, a 10 kton movable detector placed underwater. Geological setting on the HPE-depleted

oceanic crust is an ideal location: the mantle contribution to the total geoneutrino flux would be dominant, at the level of about 80% of the total signal. Thus, the principal goal of the geoneutrino measurements, determination of the mantle signal, could be reached without the complication of the subtraction of a large signal from the local crust.

For an interested reader, more comprehensive information about geoneutrinos can be found in dedicated review articles, as for example [64,65].

References

1. J.H. Davies and D.R. Davies, "Earth's surface heat flux", Solid Earth **1**, 5 (2010).
2. C. Jaupart, S. Labrosse, and J.C. Mareschal, "Temperatures, Heat and Energy in the Mantle of the Earth" in *Temperatures, Heat and Energy in the Mantle of the Earth*, ed. D.J. Stevenson (Treatise of Geophysics, Elsevier, Amsterdam, pp. 1-53, 2007).
3. G. Eder, "Terrestrial Neutrinos", Nucl. Phys. **78**, 657 (1966).
4. G. Marx, "Geophysics by neutrinos", Czech J. Phys. **B**, 19 (1969) 1471.
5. G. Marx and N. Menyhard, *Mitteilungen der Sternwarte*, Budapest No. 48 (1960).
6. G. Marx and I. Lux, "Antineutrino Luminosity of the Earth", Talk at the Moscow Conference on Neutrino Physics and Neutrino Astrophysics. *ITP-Budapest Report* 243, 1968.
7. G. Marx and I. Lux, "Hunting for Soft Antineutrinos", *Acta Phys. Hung.*, *ITP-Budapest Report* 256, 1969.
8. M. L. Krauss, S. L. Glashow, and D.N. Schramm, "Antineutrino astronomy and geophysics",Nature **310**, 19 (1984).
9. R. Raghavan, "Detecting a Nuclear Fission Reactor at the Center of the Earth", internal report of Bell Laboratories and LNG-INFN.
10. R. Raghavan *et al.*, "Measuring the Global Radioactivity in the Earth by Multidetector Antineutrino Spectroscopy", *Phys. Rev. Lett.* **80**, 635 (1998).
11. C. G. Rothschild, M. C. Chen, and F. P. Calaprice, "Antineutrino geophysics with liquid scintillator detectors", Geoph. Res. Lett. **25, 7**, 1083 (1998).
12. K. H. Wedepohl, "The Composition of the Continental Crust", Geochim. Cosmochim. Acta **59-7**, 1217 (1995).
13. R. L. Rudnick and D. M. Fountain, "Composition of the Continental Crust", Rev. Geophys. **33-3**, 267 (1995).
14. S. R. Taylor and S. M. McLennan, "The geochemical evolution of the continental crust", Rev. Geophys **33-2**, 241 (1995).
15. R.L. Rudnick and S. Gao, "The Composition of the Continental Crust" in *The Crust, vol. 3 Treatise on Geochemistry*, ed. R. L. Rudnick, (1-64, Elsevier, Oxford, 2003).
16. B. R. Hacker, P. B. Kelemenb, and M. D. Behn, "Differentiation of the continental crust by relamination", Earth Planet. Sci. Lett. **307**, 501 (2011).
17. Y. Huang *et al.*, "A reference Earth model for the heat-producing elements and associated geoneutrino flux", Geochem. Geophys. Geosys. **14-6**, 2003 (2013).
18. A. Zindler and S. Hart, "Chemical geodynamic", Ann. Rev. Earth Planet. Sci. **14**, 493 (1986).
19. W.F. McDonough and S.-S. Sun, "The Composition of the Earth", Chem. Geol. **120**, 223 (1995).
20. C.J. Allégre *et al.*. , "The chemical composition of the Earth", Earth Plan. Sci. Lett. **134**, 515 (1995).
21. M. Javoy, "The integral enstatite chondrite model of the Earth", Earth Planet. Sci. **329-8**, 537 (1999).
22. D. L. Turcotte and G. Schubert, "Geodynamics", 2nd ed, 456 pp, *Cambridge University Press*, geol. mag 139 (2002).
23. H. Palme and H. S. C. O'Neill, "Cosmochemical estimates of mantle composition" in *The Mantle and Core, vol. 2 Treatise of Geochemistry*, ed. R.W. Carlson (Elsevier, Oxford, pp.

1-38, 2003).
24. V. J. M. Salters and A. Stracke,"Composition of the depleted mantle", Geochem. Geophys. Geosys. **5-5**, Q05B07, (2004).
25. R. K. Workman and S. R. Hart, "Major and trace element composition of the depleted MORB mantle (DMM)", Earth Planet. Sci. Let. **231-1-2**, 53 (2005).
26. T. Lyubetskaya and J. Korenaga, "Chemical composition of Earth's primitive mantle and its variance.", J. Geophys. Res. **112**, B03211 (2007)
27. H. S. C. O'Neill and H. Palme,"Collisional erosion and the non-chondritic composition of the terrestrial planets", Phil. Trans. Roy. Soc. A: Math. Phys. Eng. Sci. **366**, 4205 (2008).
28. R. Arevalo, W. F. McDonough, and M. Luong, "The K/U ratio of the silicate Earth: Insights into mantle composition, structure and thermal evolution", Earth Planet. Sci. Let. **278**, 361 (2009).
29. R. Jr. Arevalo and W. F. McDonough, "Chemical variations and regional diversity observed in MORB", Chem. Geol. **271**, 70 (2010).
30. M. Javoy *et al.*, "The chemical composition of the Earth: Enstatite chondrite models", Earth Planet. Sci. Let. **293**, 259 (2010).
31. G. Fiorentini, F. Mantovani, and B. Ricci, "Neutrinos and energetics of the Earth", Phys. Lett. B **557**, 139 (2003).
32. F. Mantovani, L. Carmignani, G. Fiorentini, and M. Lissia, "Antineutrinos from Earth: A reference model and its uncertainties", *Phys. Rev.* D **69**, 0130011 (2004).
33. G. Fiorentini, M. Lissia, and F. Mantovani, "Geo-neutrinos and earth's interior", Phys. Rep. **453**, 117 (2007).
34. G. Fiorentini, M. Lissia, F. Mantovani, and R. Vannucci, "How much uranium is in the Earth? Predictions for geoneutrinos at KamLAND", *Phys. Rev.* D **72**, 033017 (2005).
35. S. T. Dye, "Geo-neutrinos and silicate earth enrichment of U and Th", Earth Planet. Sci. Let. **297**, 1 (2010).
36. M. Coltorti *et al.*, "U and Th content in the Central Apennines continental crust: A contribution to the determination of the geo-neutrinos flux at LNGS", Geochim. Cosmochim. Acta **75**, 2271 (2011).
37. Y. Huang *et al.*, "Regional study of the Archean to Proterozoic crust at the Sudbury Neutrino Observatory (SNO+), Ontario: Predicting the geoneutrino flux", Geochem. Geophys. Geosys. **15-10**, 3925 (2014).
38. V. Strati *et al.*, "Expected geoneutrino signal at JUNO", Progr. Earth Planet. Sci. **2**, 5 (2015)
39. L. Wan, G. Hussain, Z. Wang, and S. Chen, "Geoneutrinos at Jinping: Flux prediction and oscillation analysis", *Phys. Rev.* D **95**, 053001 (2017)
40. S. Enomoto, E. Ohtani, K. Inoue, and A. Suzuki, "Neutrino geophysics with KamLAND and future prospects", Earth Planet. Sci. Lett. **258**, 147 (2007).
41. G.L. Fogli, E. Lisi, A. Palazzo, and A.M. Rotunno, "Geo-neutrinos: A systematic approach to uncertainties and correlations", Earth, Moon, and Planets **99**, 111 (2006).
42. O. Šrámek *et al.*, "Geophysical and geochemical constraints on geo-neutrino fluxes from Earth's mantle", Earth Planet. Sci. Lett. **361**, 356 (2013).
43. Y. Wang and L. Wen, "Mapping the geometry and geographic distribution of a very low velocity province at the base of the Earth's mantle", J. Geophys. Res. **109 (B10)**, B10305 (2004).
44. H. K. C. Perry, J.-C. Mareschal, and C. Jaupart, "Enhanced crustal geo-neutrino production near the Sudbury Neutrino Observatory, Ontario, Canada", Earth Planet. Sci. Lett. **288**, 301 (2009).
45. J.-C. Mareschal, C. Jaupart, C. Phaneuf, and C. Perry, "Geoneutrinos and the energy budget of the Earth", J. Geodynamics **54**, 43 (2012).
46. J.-C. Mareschal, C. Jaupart, and L. Iarotski. "The Earth Heat Budget, Crustal Radio-

activity and Mantle Geoneutrinos" in "Geo-neutrinos". *Open Academic Press*, ed. Livia Ludhova, ISBN 978-83-944520-1-8.
47. A. Suzuki, "Present status of KamLAND", Nucl. Phys. B (Proc. Suppl.) **77**, 171 (1999).
48. G. Alimonti *et al.* (Borexino Collaboration), "The Borexino detector at the Laboratori Nazionali del Gran Sasso", Nucl. Instr. Meth. Phys. Ress A **600**, 568 (2009).
49. M. Baldoncini *et al.*, "Reference worldwide model for antineutrinos from reactors", *Phys. Rev.* D **91**, 065002 (2015).
50. S. Enomoto, "Neutrino Geophysics and Observation of Geo-Neutrinos at KamLAND", Ph. D. Thesis, Tohoku University, Japan, 2005.
51. T. Araki *et al.* (KamLAND Collaboration), "Experimental investigation of geologically produced antineutrinos with KamLAND", Nature **436**, 499 (2005).
52. S. Abe *et al.* (KamLAND Collaboration), "Precision Measurement of Neutrino Oscillation Parameters with KamLAND", *Phys. Rev. Lett.* **100**, 221803 (2008).
53. A. Gando *et al.* (KamLAND Collaboration), "Partial radiogenic heat model for Earth revealed by geo-neutrino measurements", Nat. Geosci. **4**, 647 (2011).
54. A. Gando *et al.* (KamLAND Collaboration), "Reactor On-Off Antineutrino Measurement with KamLAND", *Phys. Rev.* D **88**, 033001 (2013).
55. H. Watanabe *et al.* (KamLAND Collaboration), "KamLAND", *talk at Neut. Res. and Thermal Evol. Earth*, Tohoku Uni., Sendai, Japan, 2016.
56. G. Bellini *et al.* (Borexino Collaboration), "Observation of geo-neutrinos", *Phys. Lett.* B **687**, 299 (2010).
57. G. Bellini *et al.* (Borexino Collaboration), "Measurement of geo-neutrinos from 1353 days of Borexino", *Phys. Lett.* B **722**, 295 (2013).
58. M. Agostini *et al.* (Borexino Collaboration), "Spectroscopy of geoneutrinos from 2056 days of Borexino data", *Phys. Rev.* D **92**, 031101(R) (2015).
59. J.M. Herndon, "Substructure of the inner core of the Earth", Proc. Nat. Acad. Sci. USA **93**, 646 (1996).
60. M. Chen, "Geo-neutrinos in SNO^{+}", Earth, Moon and Planets **99**, 221 (2006).
61. F. An *et al.* (JUNO Collaboration), "Neutrino physics with JUNO", J. Phys. G: Nucl. Part. Phys. **43**, 030401 (2016).
62. J.F. Beacom *et al.* (Jinping Collaboration), "Physics prospects of the Jinping neutrino experiment", Chin. Phys. C **41**, 023002 (2017).
63. J. G. Learned, S.T. Dye, and S. Pakvasa, "Hanohano: A Deep Ocean Anti-Neutrino Detector for Unique Neutrino Physics and Geophysics Studies", arXiv: 0810.4975,2008.
64. G. Bellini *et al.*, "Geo-neutrinos", Prog. Part. Nucl. Phys. **73**, 1 (2013).
65. L. Ludhova and S. Zavatarelli, "Studying the Earth with Geoneutrinos", Adv. High En. Phys. **2013**, 425693 (2013).